Liquid Crystals
Publication details, including instructions for authors and subscription information:
http://www.informaworld.com/smpp/title~content=t713926090

Formation of a homochiral antiferroelectric ground state in asymmetric bent-shaped molecules

Seng Kue Lee[a]; Sungmin Kang[a]; Masatoshi Tokita[a]; Junji Watanabe[a]
[a] Department of Organic and Polymeric Materials, Tokyo Institute of Technology, O-okayama 2-12-1, Meguro-ku, Tokyo, Japan

To cite this Article Kue Lee, Seng , Kang, Sungmin , Tokita, Masatoshi and Watanabe, Junji(2010) 'Formation of a homochiral antiferroelectric ground state in asymmetric bent-shaped molecules', Liquid Crystals, 37: 5, 593 — 598

To link to this Article: DOI: 10.1080/02678291003710482

URL: http://dx.doi.org/10.1080/02678291003710482

Liquid Crystals,
Vol. 37, No. 5, May 2010, 593–598

Taylor & Francis
Taylor & Francis Group

Formation of a homochiral antiferroelectric ground state in asymmetric bent-shaped molecules

Seng Kue Lee*, Sungmin Kang, Masatoshi Tokita and Junji Watanabe

Department of Organic and Polymeric Materials, Tokyo Institute of Technology, O-okayama 2-12-1, Meguro-ku, Tokyo 152-8552, Japan

(*Received 19 January 2010; final version received 17 February 2010*)

New asymmetric bent-shaped molecules were synthesised and their mesomorphic properties and phase structures investigated by means of electro-optical measurements. All of the compounds formed fluid smectic phases and showed the homochiral antiferroelectric (SmC_AP_A) ground structure of the B2 phase. Comparing the new molecules with the previously reported classical symmetric bent-shaped molecules, we concluded that the modification of the chemical structure, especially the asymmetrical design of the bent-shaped molecules, is very significant for the interlayer interaction, influencing the formation of a specific polar order in banana phases.

Keywords: bent-shaped molecules; chirality; phase structure; (anti)ferroelectricity

1. Introduction

Since their discovery by Niori et al. [1], bent-shaped (or banana) molecules and their unconventional mesophases with a unique polarity [1] and chirality [2] have intrigued scientists and opened up a new era in liquid crystal science. A large number of molecules have been synthesised and characterised, and various examinations of switching behaviour, macroscopic chirality and optical activity have been carried out [3–5]. Among the banana mesophases, the most widely investigated phase is the B2 phase because of its (anti)ferroelectric switching behaviours. Since molecules in the B2 phase are tilted to the smectic layer, four distinct types of structure, that is, anticlinic antiferroelectric (SmC_AP_A) and synclinic antiferroelectric (SmC_SP_A), anticlinic ferroelectric (SmC_AP_F) and synclinic ferroelectric (SmC_SP_F), can be distinguished depending on the tilt direction and polar direction of the molecules in adjacent layers. The antiferroelectric state is generally the ground state. Moreover, depending on the switching current and optical microscopic measurements, most exhibit SmC_SP_A in the ground state because the end chains of molecules in this state are parallel to each other. This state is racemic and the layer chirality alters from layer to layer, while a homochiral antiferroelectric (SmC_AP_A) order is less frequently observed [6–8]. In this study, we demonstrate the results of our investigation of the mesophases of new asymmetric bent-shaped molecules, especially the formation of a homochiral antiferroelectric (SmC_AP_A) in the ground state.

2. Experimental details

2.1 Measurements

Textures were observed under a crossed polariser using an Olympus BX50 polarising optical microscope (POM) equipped with a temperature-controlled Mettler Toledo FP 90 hot stage. Transition temperatures were determined by differential scanning calorimetry (DSC) using a Perkin Elmer DSC 7 calorimeter. Electro-optic responses and polarisation reversal current were observed using a high-speed voltage amplifier (F20A, FLC Electronics, Partille, Sweden) connected to a function generator (WF1945A, NF Electronic Instruments, Yokohama, Japan). The sample was sandwiched between glass substrates with indium tin oxide electrodes and the substrate surface was neither polymer coated nor rubbed. ^1H nuclear magnetic resonance (NMR) spectra were recorded on a JEOL FT-NMR AL400 (400 MHz) spectrometer using deuterated chloroform ($CDCl_3$) as an internal standard. Elemental analysis was determined by CHN Corder MT-6.

2.2 Synthesis

The chemical structures and the synthetic routes of the target compounds are illustrated in Scheme 1. One side wing is the same as a classical bent-shaped molecule (P-12-O-PIMB) but the other side wing was changed slightly [6].

2.2.1 Synthesis of 4-formylbenzoic acid-3-methoxyphenyl ester *3*

To a solution of 3-methoxyphenol **1** (3.0 g, 24.1 mmol) in dichloromethane (CH_2Cl_2) (50 ml) was added 1,3-dicyclohexylcarbodiimide (DCC) (5.98 g, 28.9 mmol), 4-dimethylaminopyridine (DMAP) (3.54 g, 28.9 mmol), and 4-formylbenzoic acid **2** (3.62 g, 24.1 mmol). The mixture was stirred at room temperature for 2 days. After filtration to remove precipitated materials, the

---

*Corresponding author. Email: sklee@polymer.titech.ac.jp

ISSN 0267-8292 print/ISSN 1366-5855 online

DOI: 10.1080/02678291003710482
http://www.informaworld.com

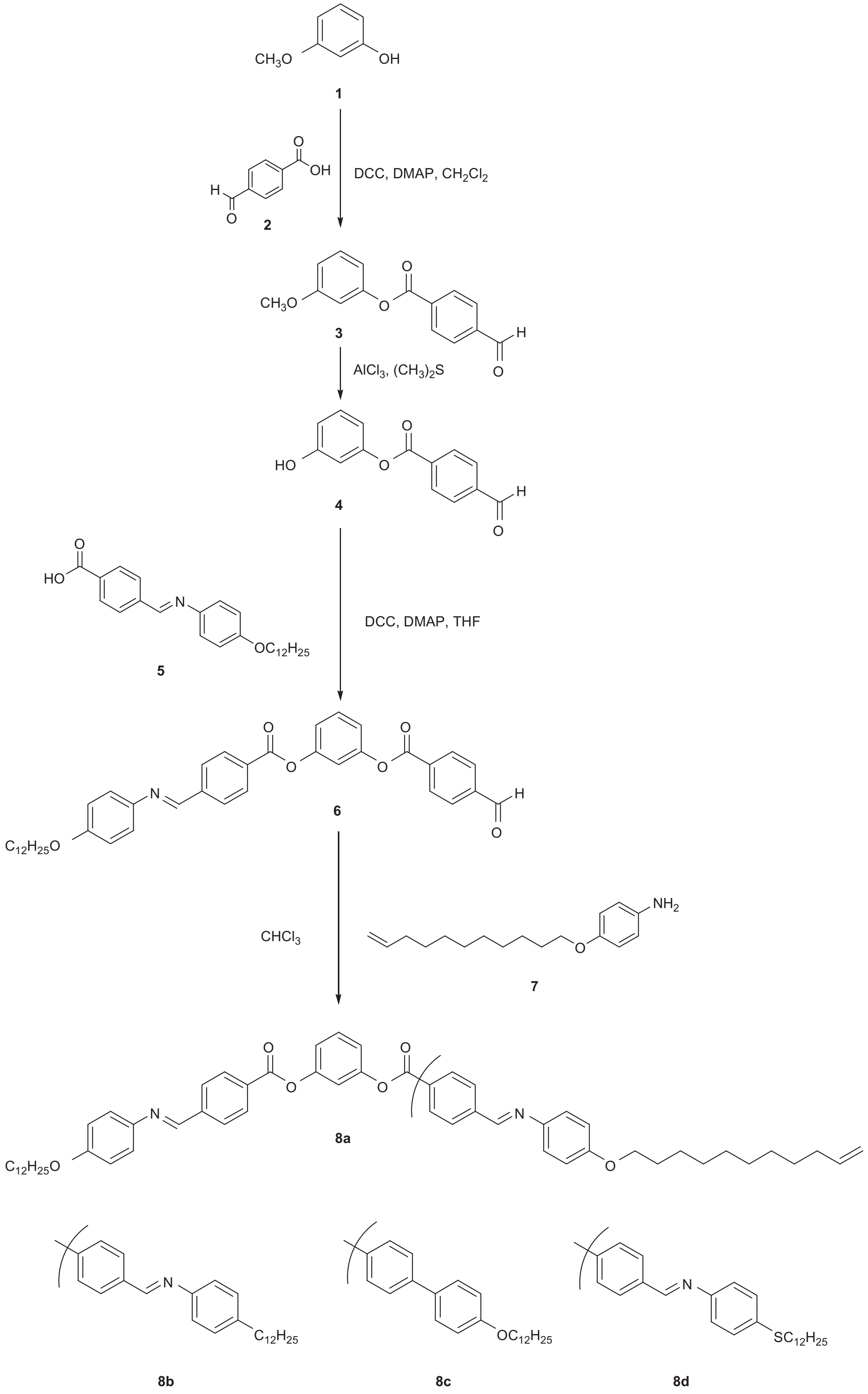

Scheme 1. The chemical structures and the synthetic routes of the target compounds.

filtrate was chromatographed on silica gel (CH_2Cl_2) and then recrystallised from CH_2Cl_2/ethanol to isolate **3** (2.54 g, 41%) as a white solid. ^{1}H-NMR (400 MHz, $CDCl_3$) δ 3.86 (s, 3H), 6.72–7.39 (m 4H), 8.02 (d, $J =$ 8.4 Hz, 2H), 8.35 (d, $J =$ 8.4 Hz, 2H), 10.1 (s, 1H).

*2.2.2 Synthesis of 4-formylbenzoic acid-3-hydroxyphenyl ester **4***

A CH_2Cl_2 (20 ml) solution of **3** (2.0 g, 7.80 mmol) was added to aluminium chloride (5.2 g, 39.0 mmol) in CH_2Cl_2 (10 ml) at 0°C. Dimethylsulphide (2.85 ml, 39.0 mmol) was then added dropwise and the resulting mixture was stirred for 1 h. Reaction was quenched by the addition of saturated aqueous ammonium chloride solution and extracted with CH_2Cl_2 (20 × 2 ml). The combined organic extracts were washed with water, dried over magnesium sulphate and concentrated. The residue was purified by column chromatography on silica gel (CH_2Cl_2) to isolate **4** (1.80 g, 95%) as a white solid. ^{1}H-NMR (400 MHz, $CDCl_3$) δ 7.20–7.55 (m 4H), 8.03 (d, $J =$ 8.4 Hz, 2H), 8.36 (d, $J =$ 8.4 Hz, 2H), 10.1 (s, 1H).

*2.2.3 Synthesis of 4-formylbenzoic acid-3-{4-[(4-dodecyloxyphenylimino)methyl]benzoyloxy}phenyl ester **6***

A mixture of 4-[(4-dodecyloxyphenylimino)methyl]-benzoic acid **5** (0.80 g, 2.06 mmol), 4-formylbenzoic acid-3-hydroxyphenyl ester **4** (0.50 g, 2.06 mmol), DCC (0.51 g, 2.47 mmol), and DMAP (0.30 g, 2.47 mmol) in tetrahydrofuran (30 ml) was stirred at room temperature for 1 day. After the reaction mixture was filtered, the solution was evaporated. The resulting solid was then recrystallised from CH_2Cl_2/ethanol to isolate **6** (0.80 g, 62%) as a yellow solid. ^{1}H-NMR (400 MHz, $CDCl_3$) δ 0.88 (t, $J =$ 6.8 Hz, 3H), 1.26–1.82 (m, 20H), 3.98 (t, $J =$ 6.8 Hz, 2H), 6.93–8.38 (m, 16H), 8.58 (s, 1H), 10.1 (s, 1H).

*2.2.4 Synthesis of 4-[(4-undec-10-enyloxyphenylimino)methyl]benzoic acid-3-{4-[(4-dodecyloxyphenyl-imino)methyl]benzoyloxy}phenyl ester **8a***

A solution of **6** (0.30 g, 0.47 mmol) and 4-undec-10-enyloxyphenylamine **7** (0.12 g, 0.47 mmol) in chloroform (20 ml) was heated under reflux for 5 h. The reaction mixture was concentrated and recrystallised from chloroform/ethanol twice to give a yellow crystal of **8a** (0.30 g, 73%). Target compounds 4-[(4-dodecylphenylimino)methyl]benzoic acid-3-{4-[(4-dodecyloxyphenylimino)methyl]-benzoyloxy}phenyl ester (**8b**), 4'-dodecyloxybiphenyl-4-carboxylic acid-3-{4-[(4-dodecyloxypheny-limino)methyl]benzoyloxy}phenyl ester (**8c**), and 4-[(4-dodecylsulfanyl-phenylimino)methyl]benzoic acid-3-{4-[(4-dodecyloxyphenylimino)methyl]benzoyloxy}phenyl ester **(8d)** were similarly prepared with 70%, 75% and 72% yield, respectively.

For **8a**, ^{1}H-NMR 0.88 (t, J = 6.8 Hz, 3H), 1.26–2.05 (m, 36H), 3.99 (t, J = 6.8 Hz, 4H), 4.92–5.01 (m, 2H), 5.76–5.86 (m, 1H), 6.93–8.29 (m, 20H), 8.58 (s, 2H). Elemental analysis: calculated for $C_{57}H_{68}N_2O_6$ C 78.05, H 7.81, N 3.19, O 10.94; found C 76.49, H 7.65, N 3.03, O 12.83.

For **8b**, ^{1}H-NMR 0.88 (t, J = 6.8 Hz, 6H), 1.20–1.63 (m, 40H), 2.63 (t, J = 7.2 Hz, 2H), 3.99 (t, J = 6.8 Hz, 2H), 6.94–8.57 (m, 20H), 8.58 (s, 2H). Elemental analysis: calculated for $C_{58}H_{72}N_2O_5$ C 79.41, H 8.27, N 3.19, O 9.12; found C 78.64, H 8.07, N 3.03, O 10.26.

For **8c**, ^{1}H-NMR 0.88 (t, J = 6.8 Hz, 6H), 1.27–1.82 (m, 40H), 3.99 (t, J = 6.8 Hz, 2H), 4.00 (t, J = 6.8 Hz, 2H), 6.94–8.30 (m, 20H), 8.58 (s, 1H). Elemental analysis: calculated for $C_{57}H_{71}NO_6$ C 79.04, H 8.26, N 1.62, O 11.08; found C 78.38, H 8.16, N 1.57, O 11.89.

For **8d**, ^{1}H-NMR 0.88 (t, J = 6.8 Hz, 6H), 1.22–1.68 (m, 40H), 2.94 (t, J = 6.8 Hz, 2H), 3.99 (t, J = 6.8 Hz, 2H), 6.93–8.30 (m, 20H), 8.56 (s, 1H), 8.58 (s, 1H). Elemental analysis: calculated for $C_{58}H_{72}N_2O_5S$ C 76.61, H 7.98, N 3.08, O 8.80, S 3.53; found C 75.82, H 7.91, N 2.96, O(+S) 13.31.

3. Result and discussion

All the asymmetric bent-shaped molecules exhibited enantiotropic transition. Mesomorphic transition temperatures and associated enthalpy changes were collected from DSC in conjunction with POM and are summarised in Table 1.

In **8a**, a typical B2 phase was observed as high birefringent circular domains on cooling from the isotropic liquid phase. On applying an electric field, the extinction direction of the circular domains rotated in an opposite direction on reversing the polarity. Figure 1 shows the switching behaviours between the two field-induced homochiral synclinic ferroelectric states (SmC_SP_F) with a homochiral anticlinic antiferroelectric ground state (SmC_AP_A) at field-off state. In this anticlinic ground state the average optical axis was parallel

Table 1. Transition temperatures (°C) and enthalpies (ΔH, kJ mol^{-1}) (in brackets) of asymmetric bent-shaped compounds (based on cooling data).

Compound	Transition temperature/°C (enthalpies/kJ mol^{-1})
8a	Iso 157.3 (17.9) B2 130.9 (31.7) B4
8b	Iso 149.3 (18.3) B2 114.4 (4.89) Cry
8c	Iso 144.9 (19.9) B2 129.4 (24.6) Cry_2 70.8 (5.85) Cry_1
8d	Iso 150.8 (21.3) B7+B2 123.3 (17.4) Cry_2 92.4 (3.90) Cry_1

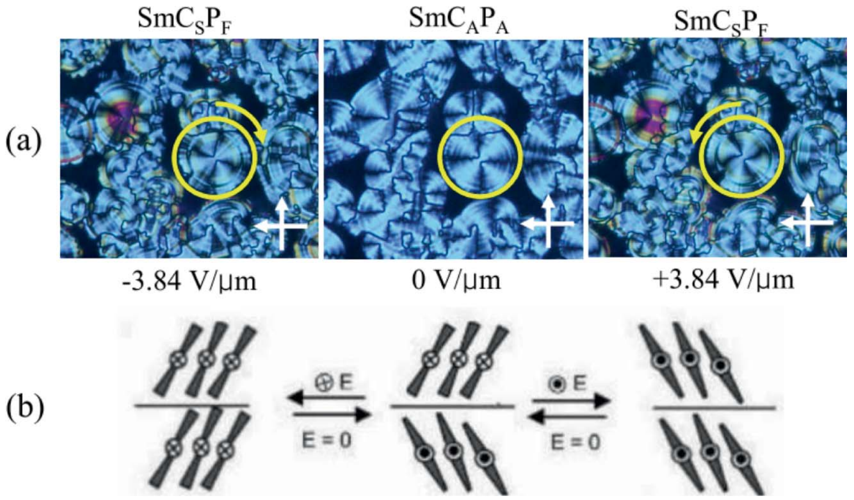

Figure 1. (a) Photomicrographs of switching behaviour in the $\mathrm{SmC_AP_A}$ phase of **8a**. (b) Schematic representation of the molecular rearrangement on antiferroelectric switching. The cell thickness is 5.2 μm.

to the polariser and analyser because of the alternation of the tilt direction, and hence the dark brushes occur parallel to the direction of the polariser. On the other hand, these brushes were inclined with the position of the polariser and analyser in the synclinic tilted phases.

On applying a triangular-wave electric field, this phase exhibited double switching current peaks in a half circle as shown in Figure 2, indicating that it has an undoubtedly antiferroelectric structure and electro-optical switching takes place between $\mathrm{SmC_AP_A}$ and $\mathrm{SmC_SP_F}$. On further cooling to the lower temperature region, a typical B4 phase with two opposite chiral domains was observed.

Compounds **8b** and **8c** also showed a homochiral anticlinic antiferroelectric ($\mathrm{SmC_AP_A}$) layer structure of the B2 phase as shown in Figure 3, but did not show the chiral segregated domains of the B4 phase in the lowest temperature region. In **8c,** two crystal phases were observed with clear transition peaks on the DSC thermogram on further cooling from the B2 phase.

When the cell was cooled from the isotropic phase in **8d**, a variety of textures, spiral, myelin-like and banana-leaf-like, to the B7 phase was observed (Figure 4(a)). Of interest is the fact that an unusual low birefringent B2 phase can also be observed in a slowly cooling condition from the isotropic phase. This type of B2 phase was characterised by showing two types of optically active domains with opposite chiral sense [9, 10]. On slow cooling (1°C min^{-1}) from the isotropic liquid, several small fractal nuclei initially appeared and then gradually combined to form large optically active domains with a low birefringence (Figure 4(b)).

This result exactly corresponds to the DSC peaks. On slow cooling (1°C min^{-1}) from the isotropic liquid,

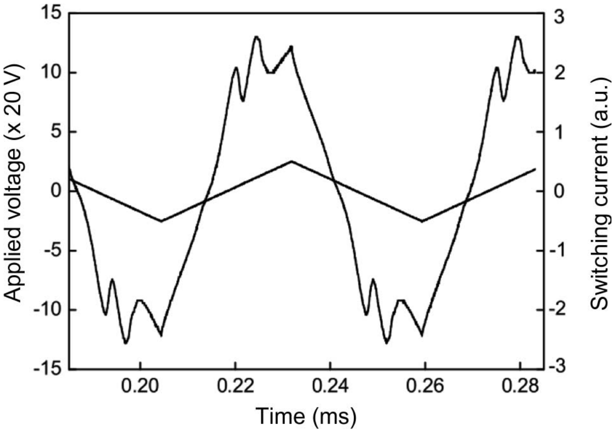

Figure 2. The polarisation reversal current in the $\mathrm{SmC_AP_A}$ phase of **8a** at 145°C under the application of 100 $\mathrm{V_{pp}}$ triangular wave voltage of 18 Hz. The cell thickness is 5.2 μm.

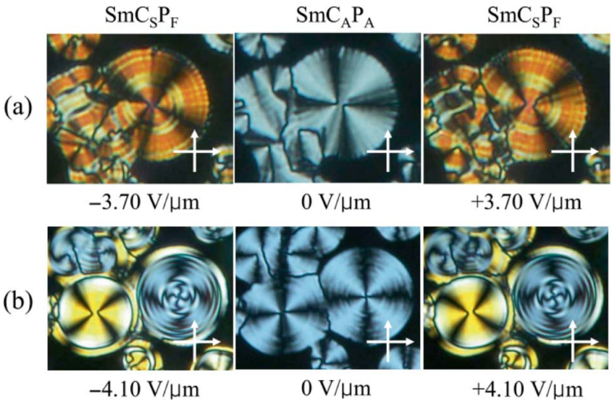

Figure 3. Photomicrographs illustrating the switching behaviour in the $\mathrm{SmC_AP_A}$ phase of (a) **8b** and (b) **8c** under the application of an electric field.

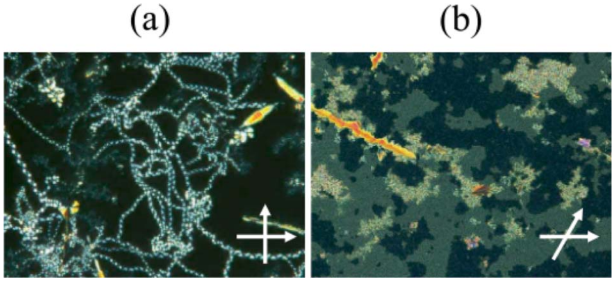

Figure 4. Photomicrographs illustrating (a) the spiral domain of a typical B7 phase and (b) a low birefringent B2 phase of **8d**, which can be observed in different places of the microscopic samples.

the peak of the B2 phase came out first and a second peak of the B7 phase appeared a little later. However, only one peak was observed on somewhat faster cooling (10°C min^{-1}), as shown in Figure 5. This result means that the energy gap between the B2 and B7 phases may be very narrow. Thus, two distinct phases may be joined in the faster cooling condition. Although more comprehensive study will be required, the flexibility of the alkylthio-terminal chain enables the compound to change conformation more easily and affects the mesophase structure in this molecule [11].

By application of an electric field, this combined texture was transformed into a relatively large domain and simultaneously two switching current peaks within a half cycle. Further, microscopic texture showed anticlinic to clinic transformation, indicating that this phase is also a homochiral antiferroelectic (SmC_AP_A) layer structure. However, this homochiral structure was transformed to a racemic (SmC_SP_A) structure when the field was continuously applied with higher voltage, in which relatively large size domains with an extinction direction parallel and perpendicular to the layer normal were observed and the characteristic stripes observed in the field-off state. This result may be caused by the weakness of the antiferroelectric ground state, especially in the chiral domains. On further cooling to the lower temperature region, two crystal phases were also observed with clear transition peaks on the DSC thermogram.

In general, in most polar smectic phases of bent-shaped molecules the ground state is antiferroelectric as mentioned above. The racemic antiferroelectric (SmC_SP_A) state especially is the most stable because of being additionally stabilized by the possibility of out-of-plane interlayer fluctuations in which the terminal chains are aligned parallel at the interlayer interface. Thus the homochiral antiferroelectric (SmC_AP_A) ground state is less frequently observed. However, both antiferroelectric ground states are energetically very similar and the formation of either SmC_AP_A or SmC_SP_A strongly rely upon the molecular structure and the experimental conditions such as surfaces and applied field, and frequently both structures coexist in one sample [8, 12]. In this study, all the asymmetric bent-shaped molecules form a homochiral antiferroelectric (SmC_AP_A) as a ground state. This result is valuable because the classical symmetric system, P-*n*-OPIMB, forms a racemic nature as a ground state [6]. This phenomenon may be constructed by a segregation of the two different side wings. Namely, the mixing of two different side wings can be energetically unfavourable because of the chemically different natures. Thus, we suggest that modification of the chemical structure, especially the asymmetrical design of bent-shaped molecules, is very significant for the interlayer interaction, influencing the formation of a specific polar order in banana phases.

4. Conclusion

We prepared new asymmetric bent-shaped molecules, in which the dodecylthio tail and typical Schiff-based

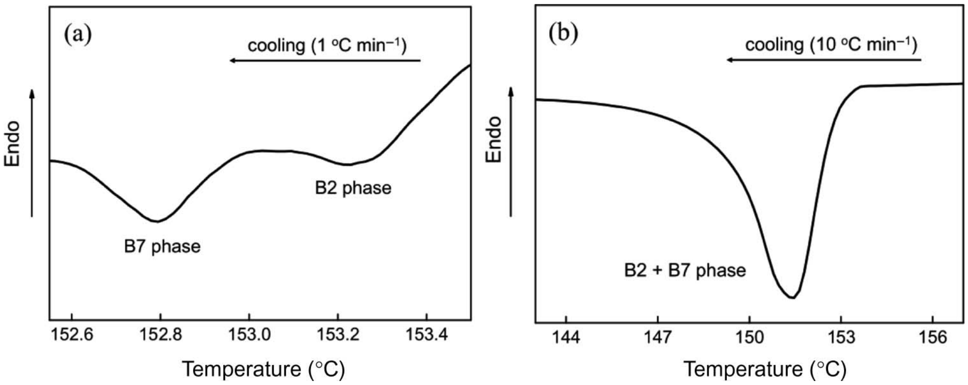

Figure 5. Differential scanning calorimetry thermograms of **8d**: (a) the peak of a B2 phase came out first and a second peak of a B7 phase appeared a little later in slowly cooling conditions (1°C min^{-1}); (b) single peak observed in somewhat faster cooling conditions (10°C min^{-1}).

side wings were substituted in one side wing, while the other side wing was changed slightly. All the asymmetric compounds formed fluid smectic phases and their mesomorphic properties were considered in terms of their molecular structure. Of interest is the fact that all compounds showed the homochiral antiferroelectric (SmC_AP_A) ground structure of the B2 phase. The formation of a SmC_AP_A structure in this system is unusual because the classical symmetric bent-shaped molecules form a racemic antiferroelectric (SmC_SP_A) layer type as a ground structure. This result indicates that the phase structure of the B2 phase strongly depends on the symmetry of the side wings. Thus, we conclude that modification of the chemical structure, especially the asymmetrical design of the bent-shaped molecules, is very significant for the interlayer interaction, influencing the formation of a specific polar order in banana phases.

Acknowledgements

This research was supported by a Grant-in-Aid for Creative Scientific Research and a Grant-in-Aid for Young Scientists B (21750138) from the Ministry of Education, Culture, Sports, Science and Technology in Japan.

References

[1] Niori, T.; Sekine, T.; Watanabe, J.; Furukawa, T.; Takezoe, H. *J. Mater. Chem.* **1996**, *6*, 1231–1233.

[2] Link, D.R.; Natale, G.; Shao, R.; Maclennan, J.E.; Clark, N.A.; Korblova, E.; Walba, D.M. *Science (Washington, DC, US)* **1997**, *278*, 1924–1927.

[3] Pelzl, G.; Diele, S.; Weissflog, W. *Adv. Mater. (Weinheim, Ger.)* **1999**, *11*, 707–724.

[4] Takezoe, H.; Takanishi, Y. *Jpn. J. Appl. Phys*. **2006**, *45*, 597–625.

[5] Reddy, R.A.; Tschierske, C. *J. Mater. Chem*. **2006**, *16*, 907–961.

[6] Nakata, M.; Link, D.R.; Thisayukta, J.; Takanishi, Y.; Ishikawa, K.; Watanabe, J.; Takezoe, H. *J. Mater. Chem*. **2001**, *11*, 2694–2699.

[7] Walba, D.M.; Körblova, E.; Shao, R.; Maclennan, J.E.; Link, D.R.; Glaser, M.A.; Clark, N.A. *Science (Washington, DC, US)* **2000**, *288*, 2181–2184.

[8] Zennyoji, M.; Takanishi, Y.; Ishikawa, K.; Thisayukta, J.; Watanabe, J.; Takezoe, H. *J. Mater. Chem*. **1999**, *9*, 2775–2778.

[9] Lee, S.K.; Shi, L.; Tokita, M.; Watanabe, J. *J. Phys. Chem. B* **2008**, *112*, 6762–6766.

[10] Lee, S.K.; Shi, L.; Tokita, M.; Takezoe, H.; Watanabe, J. *J. Phys. Chem. B* **2007**, *111*, 8698–8701.

[11] Li, X.; Lee, S.K.; Kang, S.; Tokita, M.; Kawauchi. S.; Watanabe, J. *Chem. Lett*. **2009**, *38*, 424–425.

[12] Heppke, G.; Jakli, A.; Rauch, S.; Sawade, H. *Phys. Rev. E: Stat., Nonlinear, Soft Matter Phys.* **1999**, 60, 5575–5579.